

Evolving Spatially Aggregated Features From Satellite Imagery for Regional Modeling

Sam Kriegman, Marcin Szubert, Josh C Bongard, and Christian Skalka

University of Vermont, Burlington VT 05405, USA,
sam.kriegman@uvm.edu

Abstract. Satellite imagery and remote sensing provide explanatory variables at relatively high resolutions for modeling geospatial phenomena, yet regional summaries are often desirable for analysis and actionable insight. In this paper, we propose a novel method of inducing spatial aggregations as a component of the machine learning process, yielding regional model features whose construction is driven by model prediction performance rather than prior assumptions. Our results demonstrate that Genetic Programming is particularly well suited to this type of feature construction because it can automatically synthesize appropriate aggregations, as well as better incorporate them into predictive models compared to other regression methods we tested. In our experiments we consider a specific problem instance and real-world dataset relevant to predicting snow properties in high-mountain Asia.

Keywords: spatial aggregation, feature construction, genetic programming, symbolic regression

1 Introduction

Regional modeling focuses on explaining phenomena occurring at a regional, as opposed to site-specific or global scales [11]. Regional models are of interest in many remote sensing applications, as they provide meaningful units for analysis and actionable insight to policymakers. Yet satellite imagery and remote sensing provide variables at relatively high resolutions. Consequently, studies often involve decisions concerning how to integrate this information in order to model regional processes. Considering measurements at each individual spatial unit as a separate model feature can result in a high dimensional problem in which high variance and overfitting are major concerns. For this reason, spatial aggregation is often applied in this setting to uniformly up-sample variables to be consistent with the response. Although in averaging variables across all spatial units in the region, we discard information which could in turn diminish prediction accuracy and our understanding of underlying phenomena.

Rather than strictly incorporating individual spatial units or uniformly up-sampling, it might instead be beneficial to construct features of a regional model using particularly important subsets of geographical space. In this paper, we

move away from uniform up-sampling aggregations towards more flexible and interesting aggregation operations predicated on their subsequent use as features of a regional model. We propose a novel method of inducing spatial aggregations as a component of the machine learning process, yielding features whose construction is driven by model performance rather than prior assumptions.

In experiments designed to explore these techniques, we consider a specific problem and real dataset: estimating regional Snow Water Equivalent (SWE) in high-mountain Asia with satellite imagery. Improved estimation of SWE in mountainous regions is critical [3] but is difficult due in part to complex characteristics of snow distribution [2].

2 Methods

We take a comparative approach to the SWE problem, considering ridge regression, lasso, and GP-based symbolic regression¹. For each regression model, we consider a filter-based method of feature construction in addition to a second, more dynamic method. For linear regression, we incorporate a wrapper approach in which constructed features and the regression model are induced in separate learning processes, with feedback between the two. For symbolic regression, we use an embedded approach where constructed features and the regression model are induced simultaneously over the course of an evolutionary run.

The Dataset. The SWE dataset² is derived from data collected by NASA’s Advanced Microwave Scanning Radiometer (AMSR2/E) and Moderate Resolution Imaging Spectroradiometer (MODIS) for March 1 - September 30, in 2003 - 2011, over an area that spans most of the high mountain Asia. We have three explanatory variables measured daily across a 113×113 regular grid for 1935 days: (1) mean and (2) standard deviation of sub-pixel Snow Covered Area [4, 10], as well as (3) an estimate of SWE derived from passive microwaves [15]. Our response variable is regional SWE, an attribute of the entire study region, represented as a single value for each of the 1935 days. The response was “reconstructed” by combining snow cover depletion record with a calculation of the melt rate to retroactively estimate how much snow had existed in the region [9].

2.1 Regression Models

Ridge regression [5] is similar to ordinary least squares (OLS) but subject to a bound on the L_2 -norm of the coefficients. Because of the nature of its quadratic constraint, ridge regression cannot produce coefficients exactly equal to zero and keeps all of the features in its model. Lasso (Least Absolute Shrinkage and

¹ The source code necessary for reproducing our results is available at https://github.com/skriegman/ppsn_2016.

² Raw satellite data was pre-processed by Dr. Jeff Dozier (UCSB) using previously reported techniques and is available upon request.

Selection Operator, [16]) modifies the ridge penalty and is subject to a bound on the L_1 -norm of the coefficients. The geometry of this L_1 -penalty has a strong tendency to produce sparse solutions with coefficients exactly equal to zero. In many high dimensional settings, lasso is the state-of-the-art regression method given its ability to produce parsimonious models with excellent generalization performance. For both lasso and ridge regression, the parameter constraining the coefficients is set through cross-validation.

Genetic Programming (GP, [7]) is a very flexible heuristic technique which can conveniently represent free-form mathematical equations (candidate regression models) as parse trees. GP’s inherent flexibility is well-suited for our particular problem because it can efficiently express spatial aggregations and seamlessly combine them into the learning process with minimal assumptions. Furthermore, the “white box” nature of GP may provide physical insights about this complex problem that is currently lacking, as in other domains [1, 13].

To search the space of possible GP trees we use a variant of Age-Fitness Pareto Optimization (AFPO, [12]). AFPO is a multiobjective method that relies on the concept of genotypic age, an attribute intended to preserve diversity. We extend AFPO to include an additional objective of model size, defined as the syntactic length of an individual tree. The size attribute protects parsimonious models which are less prone to overfitting the training data. The GP algorithm therefore identifies the Pareto front using three objectives (all minimized): age, error (fitness), and size. For the fitness objective, we use a correlation-based function rather than pure error, and define $f_{COR} = 1 - |\phi(\hat{s}, s)|$, where $\phi(\hat{s} - s)$ denotes Pearson correlation between model predictions (\hat{s}) and actual values of our response (s), regional SWE. Correlation has recently been shown to outperform error-based search drivers given that if a model makes a systematic error it could be easily eliminated by linearly scaling the output and therefore should be protected [14]. Accordingly, for all GP implementations, we apply a linear transformation after f_{COR} -driven evolution has concluded, by using an individual program (model) output as the single input of OLS on the training data.

Our implemented GP experiments used ramped half-and-half initialization with a height range of 2–6 and an instruction set including unary ($\{\sin, \cos, \log, \exp\}$) and binary functions ($\{\times, +, -, /\}$). One thousand individuals in the population are subject to crossover (with probability 0.75) and mutation (with probability 0.01) over the course of 1000 generations. There is a static limit on the tree height (17) as well as the tree size (300 nodes). Each experiment consists of 30 evolutionary runs, from which the best model (lowest training f_{COR}) is selected. The selected model is then transformed using OLS, and subsequently validated using unseen test data.

Standard Methods. Ridge regression, lasso, and GP may be performed on the raw data using each variable at each individual spatial unit as a separate feature. We denote these methods as Standard Ridge (SR), Standard Lasso (SL) and Standard GP (SGP). SR, SL and SGP each have access to $113 \times 113 \times 3 = 38307$ features, but only 1720 observations in each fold of data.

2.2 Feature Construction Methods

Feature construction is a well studied problem and the utility of genetic programming for feature construction has been recognized in many previous studies [8]. The key difference in our work from this past work is the nature of the data being modeled. We presume that there exist spatial autocorrelations of varying size and shape that, if aggregated to improve the signal to noise ratio, yield features supporting more accurate predictions.

In a regional model, we can construct features by aggregating higher dimensional variables across space. However, it is not entirely clear what kind of aggregations are useful as features of a predictive model. Grouping variables based on similarity or dissimilarity does not necessarily produce useful regional features. In this paper, we make an assumption about the importance of distance and continuity in effective spatial aggregations, based on Tobler’s first law of geography [17] which states that “everything is related to everything else, but near things are more related than distant things.” Accordingly, we limit the space of possible spatial aggregations to be an average of values within a circular spatial area defined by its centerpoint and radius. However, where to aggregate, how many aggregations to perform, and how to combine the aggregates must still be determined manually or decided during model optimization. We view filters and wrappers as intermediary steps in relaxing assumptions towards our embedded approach, which automates all three of these aspects.

The Filter Method. Filter-based feature construction methods transform or “filter” the original variables as a preprocessing step, prior to modeling. Our filter for the SWE problem represents a static up-sampling transformation of the original variables. Each variable is decomposed in space by a grid of overlapping circles³ of equal radii centered on a square lattice pattern of points (see Figure 2a,c,e for example). Each constructed feature corresponds to the average (arithmetic mean) of a particular variable sampled within a particular circle of space. Units that reside in an overlapping region of two separate circles are included in the calculation of both features. Since there are three explanatory variables in the SWE dataset, an $R \times R$ grid corresponds to $p = 3R^2$ constructed features. The constructed features are then used as inputs for ridge regression, lasso, and GP, which we will refer to as Filtered Ridge (FR), Filtered Lasso (FL), and Filtered GP (FGP). We will also specify the value of R used in a particular model instance as a subscript, e.g. FR_{15} denotes Filtered Ridge with $R=15$. We consider filters with $R \in \{1, 2, \dots, 20\}$, however note that the standard methods are essentially filters with $R = 113$, albeit with the non-overlapping square pixels.

The Wrapper Method. Wrapper-based feature construction methods incorporate feedback from the fit of the model. We implement wrappers around both

³ The shape of circles are in reality so-called “small circles,” as they lie on the surface of earth.

ridge regression and lasso in order to enable the circular sampling regions to define their own center and radius. The circles are no longer fixed on a grid with a predetermined size. Instead, each constructed feature is uniquely parameterized by the coordinates of a center unit (x, y) , as a latitude and longitude tuple, and a radius r , as a single value floating point number in km. The center can be any spatial unit in the region, including one at the edge of the raster. The radius is restricted to be within 0 and 1000 km, which is flexible enough to contain only a single unit or span the entire region (see Figure 2b,d for example).

Wrapped Ridge (WR) and Wrapped Lasso (WL) separately use a ridge/lasso-driven hill climbing algorithm to construct features that minimize Mean Absolute Error (MAE), i.e. $\frac{1}{n} \sum_{i=1}^n |\hat{s}_i - s_i|$, where s_i is the actual value of our response (regional SWE) and \hat{s}_i is output predicted by the model over n observations. The algorithm uses the same number of circles for each of the three variables, initializing their parameters (x, y, r) randomly. For 1000 iterations, a single constructed feature (circle) is randomly selected and subject to a Gaussian mutation on one of its parameters with standard deviation equal to 25% of the radius and centered at zero. A new ridge/lasso model is then refit on the mutated set of features using a random subset of data sampled without replacement. If the mutation lowered model error on the complementing set of training data left out, then the change is accepted. Otherwise, the mutation is undone. If a proposed mutation to the radius would take it outside the restricted range of 0 – 1000 km, then it is “bounced-back” the distance it would have exceeded the boundary. For example, a random mutation that would result in a radius of 1200 km, becomes $1000 - (1200 - 1000) = 800$ km. Thirty restarts are used from which the best model based on training data is selected. We consider $R \in \{1, 2, 3, 4\}$ for wrappers corresponding to $3 \times R^2$ features which really means $3 \times 3 \times R^2$ modifiable parameters.

The Embedded Method. By using GP, we can allow for flexibility with respect to the placement and number of aggregations as well as the way in which they are combined to form a model. However, stochastic optimization methods like GP cannot be easily “refit” in the same manner as deterministic algorithms like ridge regression or lasso. Therefore using wrapper approach for GP is computationally infeasible. Instead, modifications to aggregated features are implemented through mutation-based operators.

In Genetic Programming with Embedded Spatial Aggregation (GPESA) introduced here, our constructed features are represented as parameterized tree terminals, with parameters (x, y, r) (Figure 1). Constructed features are randomly initialized in the same manner as the wrapper method, but separately for each terminal of each individual in the population. Greedy Gaussian mutations to the parameters (x, y, r) of a randomly selected constructed feature occur in the population with 20% probability, each generation. Mutations to r have mean zero and a standard deviation of 25%, subject to the bounce-back rule. Similarly, mutations to (x, y) have mean distance zero and a standard deviation of $0.25r$. For 25 iterations, greedy mutations modify the parameterized terminals

within a particular GP tree. A modification is accepted if it successfully reduces average error (f_{COR}) on random subsets of training data sampled with replacement. Aside from the stochastic application, another key difference between the wrapper method’s hill climbing algorithm and the GPESA’s greedy mutations is that the overall regression model stays the same between mutations rather than being “refit” after each mutation.

Validation. In order to validate the generalization of models we partition the dataset into nine overlapping folds. Each fold corresponds to leaving out one year for testing and training on the remaining eight (using years 2003 - 2011). We use MAE on the unseen test data as a metric to assess model performance. To account for a difference in scale across any set of features, all input model features are standardized over time by removing the mean and scaling to unit variance. This means that as wrapper and embedded methods construct new aggregations, the sampled data is scaled over time prior to being averaged over space. Since our goal is near-real-time estimation for a future day, the training values of a feature’s mean and variance are reapplied when scaling the same feature in validation.

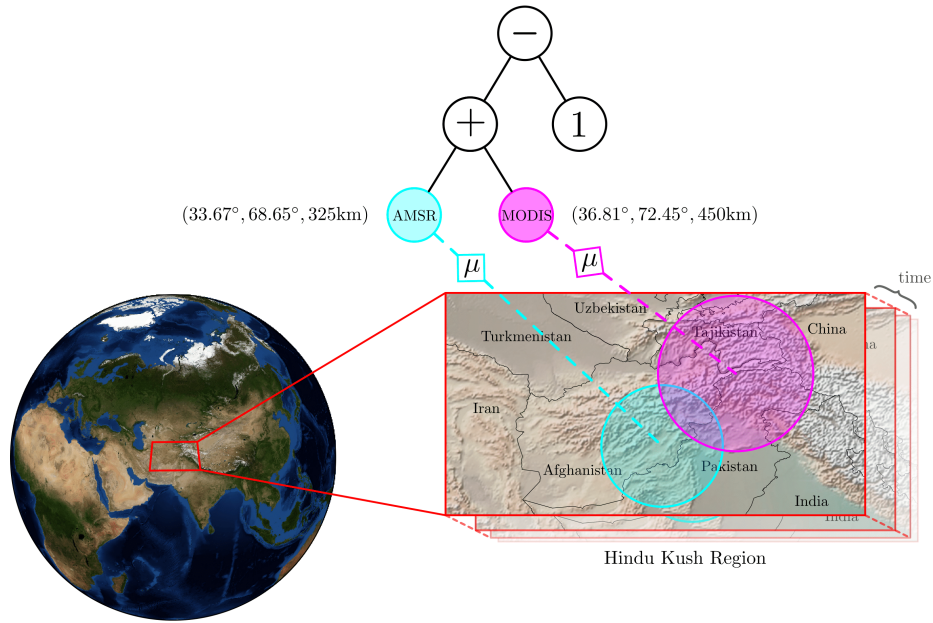


Fig. 1. In GPESA, standard GP terminals are replaced with specialized aggregation operators that allow for the automation of the number, location and size of aggregations, and the way in which they are combined to form a predictive model. Here, two such aggregations, taken from the evolved cyan and magenta regions (specified by their latitude, longitude and radius), are combined and adjusted by a scalar value.

3 Results

Table 1 displays the test error of each valid regression and feature construction method combination. For filters and wrappers, only the best performing model is displayed and we indicate the particular value of parameter R as a subscript. Since the ultimate goal of our paper is to synthesize a method better than existing approaches, we must statistically compare GPESA to SL, the state-of-the-art linear regression / variable selection algorithm. The null hypothesis of interest here is that of no difference between GPESA and a SL. Therefore we perform yearly Wilcoxon signed rank tests [6] comparing GPESA to SL with Bonferroni correction across the nine years. For five out of the nine test years, GPESA is significantly better than SL, while for the other four years there is no significant difference with SL.

Table 1. Median mean-absolute error with corresponding standard errors in parentheses. Only the best testing filter- and wrapper-based results (choice of R) are displayed. We explicitly compare GPESA with the state-of-art, SL. Bold values indicate significance (at 0.05 level with Bonferroni correction) under a Wilcoxon signed rank test in which the null hypothesis asserts that distribution of the differences between GPESA and SL is symmetrically distributed about 0.

Year	SR	SL	SGP	FR ₄	FL ₁₉	FGP ₁₉	WR ₂	WL ₃	GPESA
2003	0.86	0.51	0.35 (0.14)	0.50	0.46	0.44 (0.08)	0.43 (0.10)	0.49 (0.09)	0.29 (0.09)
2004	0.47	0.30	0.32 (0.10)	0.34	0.29	0.26 (0.05)	0.37 (0.16)	0.35 (0.16)	0.17 (0.05)
2005	0.95	0.44	0.50 (0.13)	0.61	0.40	0.52 (0.06)	0.58 (0.11)	0.63 (0.09)	0.32 (0.07)
2006	0.66	0.27	0.41 (0.29)	0.57	0.52	0.36 (0.06)	0.53 (0.11)	0.54 (0.11)	0.27 (0.05)
2007	0.72	0.33	0.44 (0.10)	0.42	0.38	0.34 (0.05)	0.52 (0.13)	0.50 (0.11)	0.24 (0.06)
2008	1.46	0.46	0.60 (0.13)	0.71	0.64	0.58 (0.11)	0.70 (0.31)	0.54 (0.26)	0.52 (0.18)
2009	0.81	0.41	0.65 (0.08)	0.90	0.61	0.56 (0.08)	0.98 (0.10)	1.03 (0.09)	0.41 (0.10)
2010	0.62	0.48	0.44 (0.12)	0.43	0.47	0.41 (0.06)	0.43 (0.11)	0.52 (0.11)	0.32 (0.07)
2011	0.87	0.48	0.61 (0.17)	0.77	0.60	0.53 (0.10)	0.82 (0.20)	0.93 (0.16)	0.45 (0.12)
Mean	0.82	0.41	0.48	0.58	0.49	0.44	0.58	0.61	0.33

Through displaying only the best testing filters and wrappers, we aim to focus speculation about GPESA performance through a conservative lens. Yet we ultimately view filters and wrappers as intermediary steps “working up” to GPESA. Accordingly, the best test error better represents a bound on the potential performance of a particular intermediary method even though it may not be possible to achieve such performance through a parameter sweep based on the training data. And indeed, across all methods tested, GPESA reported the lowest recorded median mean-absolute error within all but two years (7 of 9) where it has the second lowest.

4 Discussion

Our results show that incorporating dynamic aggregations of higher resolution variables into a regional model is beneficial in our particular problem setting, as compared to both uniform up-sampling of variables and a state-of-the-art linear regression technique (SL) that incorporates individual spatial units. SL achieves competitive prediction performance through a sparse linear combination of the individual spatial units, on par with SGP which is not linearly constrained. Ultimately, GPESA performed significantly better (lower median test error) than SL on a majority (5 of 9) of cross validation folds. Moreover, whenever GPESA was not significantly better than SL it was not significantly worse.

A main reason why GPESA has an advantage in this application is the difficulty of knowing a priori what the most important spatial datapoints are, and how to best aggregate them. Additionally, the structure of the model itself is unknown and it depends on the resulting aggregations. Therefore this is not a fixed length optimization problem, which makes it well-suited for GPESA, which can search over different numbers and non-linear combinations of spatial aggregations. While SL can theoretically perform the same aggregation as a GPESA terminal (mean within a radius of a geographical point), SL is restricted to a single linear solution while GPESA is not.

However, it’s important to emphasize that the computational cost of GPESA is higher than that of traditional GP and much higher than that of linear regression. In particular, the most expensive operation is the “on the fly” aggregation component of GPESA which makes the fitness evaluation require 500% more time than in SGP. Part of the incurred cost is due to inefficiencies of our implementation that necessitated a copy with all spatial aggregation operations. In future work we will look at reducing this overhead through more efficient data structures (e.g. k-d trees).

Importance of Spatial Data. To better understand the relevance of particular spatial locations, we define the *importance* of a spatial unit for both linear and symbolic methods, separately. For ridge regression and lasso, we can define importance by exploiting the disposition of coefficients to be larger for variables with a stronger correlation to the response, relative to a particular feature set. We define linear regression importance of a particular spatial unit as the average absolute coefficient of features that incorporate the unit into a regression model. While we cannot as easily determine relative importance within nonlinear models, we can instead define importance by exploiting the multiple candidate solutions provided from stochastic multiobjective optimization. We define GP importance of a particular spatial unit as the average absolute correlation ($1 - f_{COR}$) of nondominated solutions that incorporate the unit.

To visualize the importance of spatial information, we generated a series of heatmaps (Figure 2). In Figures 2a, 2c, and 2e we show regional importance values of filter methods for each $R \in \{1, \dots, 20\}$, with the relevant value of R annotated in the upper left corner of each box. Note that in lasso- and GP-based approaches, some variables are unused (white), while ridge cannot perform

variable selection and uses all. Figures 2b and 2d plot WR and WL for $R \in \{1, 2, 3, 4\}$. Finally, Figures 2e and 2f plot the importance of spatial information in the GP sense, for FGP and GPESA, respectively. Overall, this visualization indicates an agreement among all methods on the relatively higher importance of information in the lower center/right region of the image.

5 Conclusion

In this work we developed a novel method to address the problem of modeling a regional response with high resolution satellite imagery. We moved away from uniform up-sampling aggregations towards more flexible and interesting aggregation operations predicated on their subsequent use as features of a regional model. Our proposed technique, GPESA, is general and intended to apply to a variety of modeling problems on spatially organized data. But as an application example, and as a setting in which to evaluate our techniques, we considered the problem of estimating snow water equivalent in high mountain Asia using satellite imagery. Our results showed that using GP to evolve spatial aggregations outperforms lasso, the state-of-the-art method for directly incorporating individual spatial units into a sparse linear model.

In future work we plan to explore more flexible spatial and temporal aggregations for more predictive modeling in real earth science applications.

Acknowledgements: Thanks to Dr. Jeff Dozier (UCSB) for posing the high-mountain Asia SWE problem and providing associated datasets.

References

1. J. Bongard and H. Lipson. Automated reverse engineering of nonlinear dynamical systems. *Proceedings of the National Academy of Sciences*, 104(24):9943–9948, 2007.
2. D. Buckingham, C. Skalka, and J. Bongard. Inductive learning of snowpack distribution models for improved estimation of areal snow water equivalent. *Journal of Hydrology*, 524:311–325, 2015.
3. J. Dong, J. P. Walker, and P. R. Houser. Factors affecting remotely sensed snow water equivalent uncertainty. *Remote Sensing of Environment*, 97(1):68–82, 2005.
4. J. Dozier, T. H. Painter, K. Rittger, and J. Frew. Time-space continuity of daily maps of fractional snow cover and albedo from MODIS. *Advances in Water Resources*, 31(11):1515–1526, 2008.
5. A. E. Hoerl and R. W. Kennard. Ridge regression: biased estimation for nonorthogonal problems. *Technometrics*, 12(1):55–67, 1970.
6. M. Hollander, D. A. Wolfe, and E. Chicken. *Nonparametric statistical methods*. John Wiley & Sons, 2013.
7. J. R. Koza. *Genetic Programming: On the Programming of Computers by Means of Natural Selection*. MIT Press, Cambridge, MA, USA, 1992.
8. K. Krawiec. Genetic programming-based construction of features for machine learning and knowledge discovery tasks. *Genetic Programming and Evolvable Machines*, 3(4):329–343, 2002.

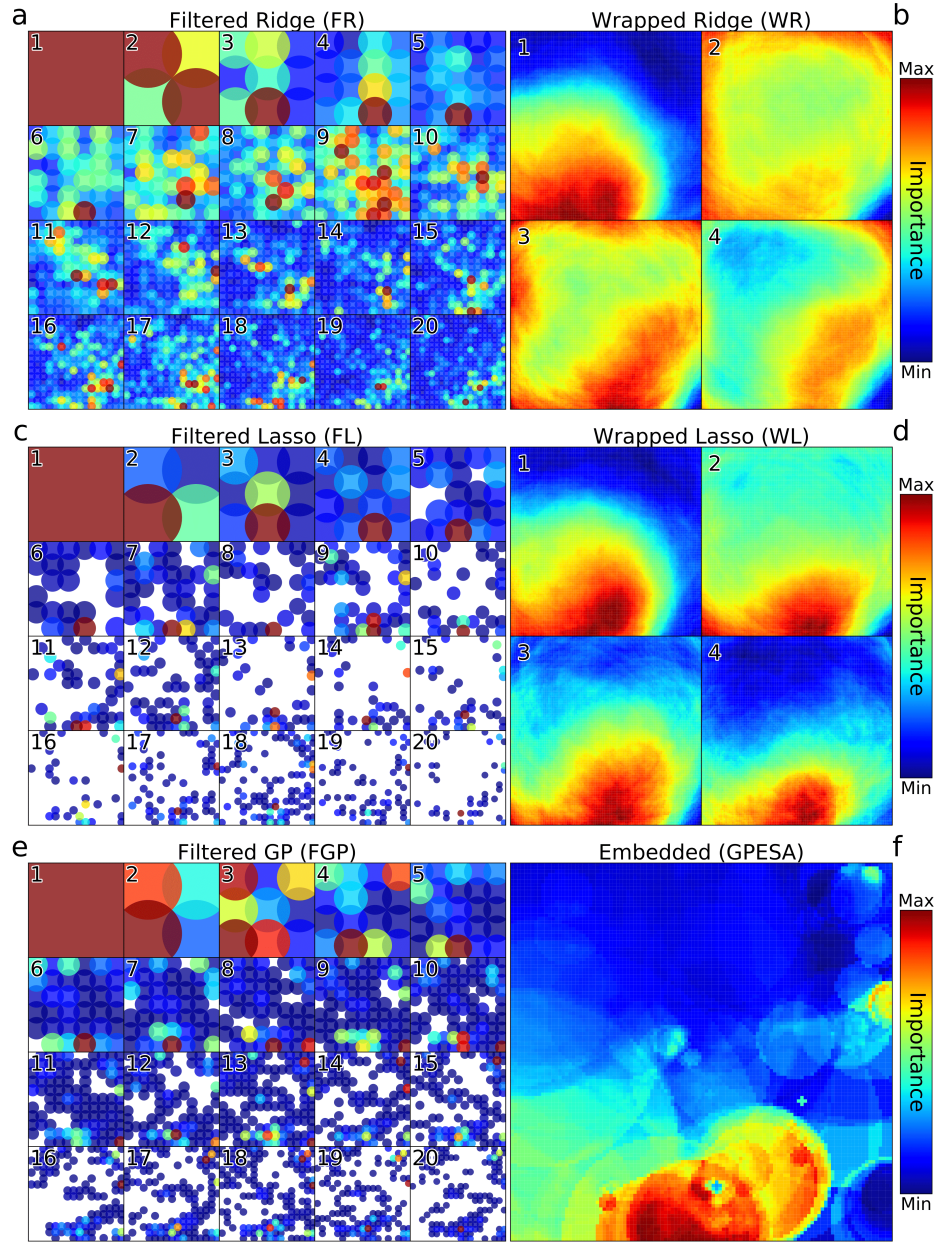


Fig. 2. Importance (defined in Section 4) of spatial units. For filters a.) FR, c.) FL, and e.) FGP, importance is displayed at each resolution $R \in \{1, 2, \dots, 20\}$ and each individual filter subplot is annotated with the corresponding R . For wrappers b.) WR and d.) WL, $R \in \{1, 2, 3, 4\}$. Finally, f.) GPESA, which has no R parameter. White areas indicate spatial units unused in feature construction across all three exploratory variables.

9. J. Martinec and A. Rango. Areal distribution of snow water equivalent evaluated by snow cover monitoring. *Water Resour. Res.*, 17(5):1480–1488, 1981.
10. T. H. Painter, K. Rittger, C. McKenzie, P. Slaughter, R. E. Davis, and J. Dozier. Retrieval of subpixel snow-covered area, grain size, and albedo from MODIS. *Remote Sensing of Environment*, 113:868–879, 2009.
11. J. Rees, A. Gibson, M. Harrison, A. Hughes, and J. Walsby. Regional modelling of geohazard change. *Geological Society, London, Engineering Geology Special Publications*, 22(1):49–63, 2009.
12. M. Schmidt and H. Lipson. Age-fitness pareto optimization. In R. Riolo, T. McConaghy, and E. Vladislavleva, editors, *Genetic Programming Theory and Practice VIII*, volume 8 of *Genetic and Evolutionary Computation*, pages 129–146. Springer New York, 2011.
13. M. D. Schmidt, R. R. Vallabhajosyula, J. W. Jenkins, J. E. Hood, A. S. Soni, J. P. Wikswo, and H. Lipson. Automated refinement and inference of analytical models for metabolic networks. *Physical biology*, 8(5):055011, 2011.
14. K. Stanislawska, K. Krawiec, and T. Vihma. Genetic programming for estimation of heat flux between the atmosphere and sea ice in polar regions. In *Proceedings of the 2015 on Genetic and Evolutionary Computation Conference*, pages 1279–1286. ACM, 2015.
15. M. Tedesco and P. S. Narvekar. Assessment of the nasa amsr-e swe product. *Selected Topics in Applied Earth Observations and Remote Sensing, IEEE Journal of*, 3(1):141–159, 2010.
16. R. Tibshirani. Regression shrinkage and selection via the lasso. *Journal of the Royal Statistical Society. Series B (Methodological)*, pages 267–288, 1996.
17. W. R. Tobler. A computer movie simulating urban growth in the detroit region. *Economic geography*, pages 234–240, 1970.